Available online at www.sciencedirect.com
SCIENCE DIRECT
Polymer 46 (2005) 10035–10044
polymer
www.elsevier.com/locate/polymer

# Effect of helix-coil transition on association behavior of both-ends hydrophobically-modified water-soluble polypeptide

Katsuhiro Inomata*, Masako Kasuya, Hideki Sugimoto, Eiji Nakanishi

*Department of Materials Science and Engineering, Nagoya Institute of Technology, Gokiso-cho, Showa-ku, Nagoya 466-8555, Japan*

Received 15 June 2005; received in revised form 5 August 2005; accepted 16 August 2005
Available online 1 September 2005

**Abstract**

Dodecyl and dodecanoyl groups (C12) are attached at the chain ends of poly[$N^5$-(2-hydroxyethyl) L-glutamine] (PHEG), and association behavior of this both-ends hydrophobically modified water soluble polypeptide (C12–PHEG–C12) has been investigated by means of light scattering measurements. Water/ethylene glycol (EG) mixed solvents were used as selective solvent for PHEG block, and PHEG changed its structure from random-coil state to α-helix with increasing EG content in the mixed solvent ($W_{EG}$). When $W_{EG}$ is less than 0.5, flower-like micelle with C12 associated core and PHEG corona in loop conformation was suggested to be formed. Increase of $W_{EG}$ from 0.5 to 0.6 induced drastic increase of association number and size of the associate, in which many C12 associated cores may be connected by PHEG in bridge conformation. This structure change of associate is considered to be driven by the increase of helix content of PHEG with $W_{EG}$, which enhances the possibility to form bridge conformation because of its rigidity. Solution preparation method, i.e. order of addition of solvent, was found to influence the structure of associate, although its effect on the helix content of PHEG was negligible.


*Keywords:* Helix-coil transition; Association; Poly[$N^5$-(2-hydroxyethyl) L-glutamine]

## 1. Introduction

ABA triblock copolymer having long middle B block and short A blocks is widely used as thermoplastic elastomers, in which A blocks form hard microdomains by microphase separation, and the A domains and B chains acts as cross-linking point and bridging chain, respectively. In a selective solvent, which is a good solvent for B block and a poor or bad solvent for A block, the ABA triblock copolymer forms associate or micelle as a consequence of association of poorly-soluble A block [1–17]. When the polymer concentration is very low and copolymer forms isolated flower-like micelles, all the B chains take loop conformation with the both-ends A blocks incorporated in same associated micellar core. With the increase of copolymer concentration, probability that respective A blocks in one copolymer are incorporated in different associated cores will increase. In this case, the middle B block can possibly take two conformations: One is loop conformation as like that in the isolated micelle, and the other is bridge conformation that connects two different associates. The increase of bridge conformation will induce formation of organized network or gel [18–35] with the associate of A chains as cross-linking point and B chain as the bridge connecting the cross-linking points. This physical gel can be regarded as a transient network [36–41], in which the cross-links are easily generated and destructed. Mechanical properties of the gel depend on number of bridging chain because loop chains are elastically ineffective.

In our previous work, micellization and gelation behavior of dilute and moderately concentrated 1-butanol solutions of poly(methyl methacrylate)-*block*–poly(*tert*-butyl acrylate)-*block*–poly(methyl methacrylate) (PMMA–PtBuA–PMMA) have been investigated [18]. 1-Butanol is good and poor solvent for PMMA and PtBuA block, respectively. $^1$H NMR, light scattering, and viscoelastic measurements at various temperature revealed that micellization and sol–gel transition have relation with segregation of terminal PMMA blocks. In this physical gel, formation of the transient network was suggested because master curves

* Corresponding author.
*E-mail address:* inomata.katsuhiro@nitech.ac.jp (K. Inomata).

0032-3861/$ - see front matter © 2005 Elsevier Ltd. All rights reserved.
doi:10.1016/j.polymer.2005.08.049

of dynamic moduli revealed Maxwell-type viscoelasticity with narrow relaxation time distribution. Concentration dependency of plateau modulus is stronger than theoretically expected, means macroscopic transient network grows with polymer concentration by increasing fraction of elastically effective bridging PtBuA chain above sol–gel transition concentration. Similar transient network is also proposed for associative water-soluble polymers such as both-ends hydrophobically modified poly(ethylene oxide) (HEUR), which have been widely used for application purpose [30–35].

Possibility to form loop conformation for ABA type copolymer should depend on chain rigidity of middle B chain. Khalatur et al. [42] presented molecular dynamic study of semiflexible telechelic polymer with associating end-groups. Their simulation results showed that flexible telechelic chain forms relatively small flower-like micelles, and for semiflexible chains, associated cores were bridged with a bundle, in which semiflexible chains are oriented in parallel to each other. Probability of loop conformation was decreased with the increase of Kuhn segment length for the middle chain. Because elasticity of physical gel of ABA-type associative copolymer depends on fraction of bridge conformation, control of chain stiffness of B block should be one of ways to control mechanical properties of the gel.

Recently, we have investigated association behavior of diblock copolymer containing water soluble non-ionic polypeptide, poly[$N^5$-(2-hydroxyethyl) L-glutamine] (PHEG) [43]. PHEG is known to take random-coil conformation in pure water and to change to α-helix structure with increasing alcohol content of the solvent [44–47]. In order to consider an effect of chain rigidity of B chain on association and gelation behavior of ABA triblock copolymer, PHEG is a suitable candidate as B block.

In this study, we have prepared both-ends hydrophobically modified PHEG as associative ABA type triblock copolymer (C12–PHEG–C12, Fig. 1), and report its association behavior in dilute solution of water/ethylene glycol (EG) mixed solvent. Dodecyl and dodecanoyl chains (C12) were used as hydrophobic alkyl chains. Helix-coil transition of PHEG chain can be induced by changing composition of the mixed solvent. Formation of micelles and its structure were investigated by using fluorescence spectroscopy and light scattering techniques. Relationship between α-helix content of middle PHEG chain and micellar structure will be described.

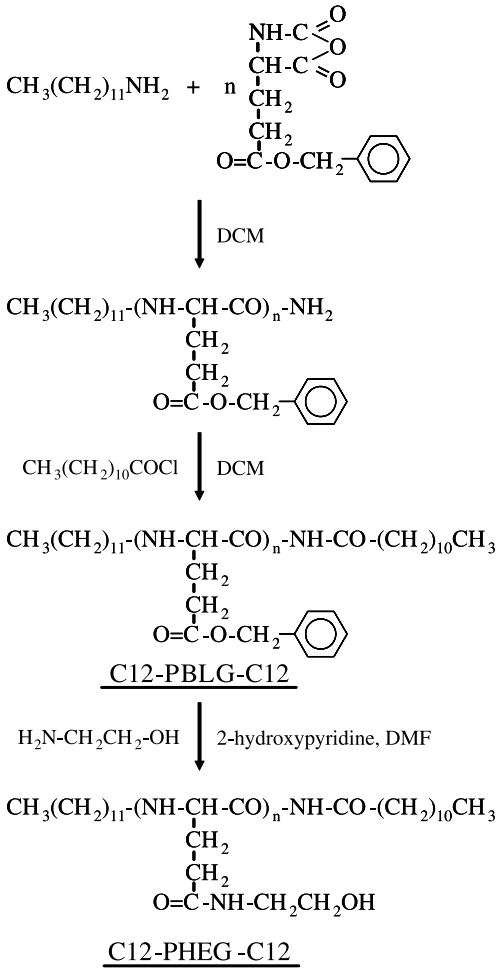


Fig. 1. Synthesis of C12–PHEG–C12.

## 2. Experimental section

### 2.1. Materials

Dodecylamine, 2-aminoethanol, 2-hydroxypyridine, and ethylene glycol (EG) was fractionally distilled before use. Dodecanoyl chloride was used as received. *N*-Carboxyanhydride (NCA) of γ-benzyl L-glutamate (BLG) was prepared by reacting BLG with triphosgene, and purified by recrystallization from tetrahydrofurane/petrorium ether. Distilled water was ion-exchanged before use.

### 2.2. Synthesis of C12–PHEG–C12

Synthetic scheme of C12–PHEG–C12 is represented in Fig. 1. NCA of BLG was polymerized with using dodecylamine in dry dichloromethane (DCM) at room temperature for 4 days. The solution was poured into diethyl ether, and the precipitates were dissolved in dry DCM containing triethylamine. This solution was cooled on ice–water bath, added excess dodecanoyl chloride slowly, and stirred at room temperature for 1 day. The reaction mixture was poured into cold methanol, and precipitates were filtered and washed with diethyl ether. The crude product was re-precipitated by DCM/methanol in order to remove unreacted reagents. The obtained C12–PBLG–C12 (Fig. 1) and 2-hydroxypyridine (5-fold molar) was dissolved in *N*,*N*-dimethylformamide (DMF), 20-fold molar amount of 2-aminoethanol was added, and side-chain exchanging reaction was performed for 24 h at 26 °C [48]. The reaction solution was neutralized by acetic acid/methanol (1/1 in

volume), and dialyzed against water by using cellulose membrane with nominal fractional molecular weight of 3500. C12–PHEG–C12 was obtained after freeze–drying of aqueous polymer solution.

### 2.3. Measurements

$^1$H NMR spectrum of C12–PHEG–C12 was recorded on a JNM-GX400 (JEOL) with using DMSO-$d_6$ as solvent. Size exclusion chromatography (SEC) chart was recorded on a SC-8020 (TOSO). Eluent solvent was DMF/LiBr (1 wt%), and standard polystyrene was used for molecular weight calibration. Circular dichroism (CD) measurements were performed on a J-820/805 (JASCO) with using a quartz cell having path length of 1 mm. Polymer concentration of the solution was ca. $8\times10^{-4}$ g/ml, and solution temperature was maintained at 30 °C. Fluorescence spectrum was measured on a RF-5300FC spectrophotofluorometer (Shimadzu) at room temperature, in order to evaluate a critical micellar concentration (CMC) of C12–PHEG–C12. 1-Anilino-8-naphthalen sulfonic acid magnesium salt (ANS-Mg, concentration: $1.6\times10^{-6}$ M) was used as fluorescence probe [49]. An excitation wavelength of 350 nm was employed for the measurements.

Static and dynamic light scattering (SLS and DLS, respectively) was measured by a laboratory-made apparatus equipped with an ALV/SO-SIPD detector and an ALV-5000 correlator using He–Ne laser (the wavelength $\lambda_0=633$ nm) as a light source [50,51]. Sample solutions were optically purified by a Millipore filter of nominal pore size of 0.45 or 1.0 $\mu$m and transferred into optical tube, and the tube was flame-sealed under gentle vacuum. Excess Rayleigh ratio $R(\theta)$ was calculated from the measured excess scattered-light intensity at different scattering angle, $\theta$, in a range of 30–120°. Conventional data analysis for SLS results by extrapolating to dilute limit was not applied because of a possibility of concentration dependence of association behavior, therefore, evaluated weight-averaged molecular weight ($M_w$) and radius of gyration ($R_g$) are apparent ones defined by the following equations.

$$M_{w,app} = \frac{R(0)}{Kc} \tag{1}$$

$$R^2_{g,app} = \frac{3\lambda_0 M_{w,app}(\text{initial slop})}{16\pi^2 n^2} \tag{2}$$

$Kc/R(0)$ and (initial slope) are intercept and initial slope of $Kc/R(\theta)$ vs. $\sin^2(\theta/2)$ plots at a finite concentration, $c$. Optical constant $K$ is defined by

$$K = \frac{4\pi^2 n^2 (\mathrm{d}n/\mathrm{d}c)^2}{N_A \lambda_0^4} \tag{3}$$

where $n$ the refractive index of solvent and $N_A$ the Avogadro constant. The refractive index increment $\mathrm{d}n/\mathrm{d}c$ was measured by a differential refractometer RM-102 (Union Giken) with using water/EG mixed solvent at different EG weight fraction ($W_{EG}$), and expressed as follows:

$$\frac{\mathrm{d}n}{\mathrm{d}c}(\text{ml/g}) = 0.1562 - 0.1566W_{EG} + 0.0988W_{EG}^2 - 0.0046W_{EG}^3 - 0.0137W_{EG}^4 \tag{4}$$

In DLS measurements, correlation function, $g^{(1)}(q, t)$, of electric field was calculated from autocorrelation function, $g^{(2)}(q, t)$, of scattered light intensity by the equation

$$g^{(2)}(q,t) = A[1 + B|g^{(1)}(q,t)|^2] \tag{5}$$

where $A$ and $B$ are constants, and $q$ is defined as $q = (4\pi n/\lambda_0)\sin(\theta/2)$. Decay function $g^{(1)}(q, t)$ was analyzed by Laplace inversion program CONTIN to evaluate decay rate ($\Gamma$) distribution. Hydrodynamic radius $R_h$ was calculated by the Einstein–Stokes equation,

$$R_h = \frac{kT}{6\pi\eta D} = \frac{kT}{6\pi\eta(\Gamma/q^2)} \tag{6}$$

where $D=\Gamma/q^2$ the diffusion coefficient, $k$ the Boltzmann constant, and $T$ the absolute temperature. The solvent viscosity $\eta$ was derived from Ref. [52]. Solution temperature was maintained at 30 °C during the measurement. Unless specifically mentioned below, sample solutions for CD, fluorescence spectroscopy, and light scattering measurements were prepared by dissolving the polymer in water/EG mixed solvent, which had been prepared at desired $W_{EG}$ in advance.

## 3. Results

### 3.1. Polymer synthesis

C12–PHEG–C12 was synthesized by aminolysis reaction of benzyl ester side chains of C12–PBLG–12 with 2-aminoethanol. De Marre et al. [48] tried to optimize condition for the aminolysis reaction of PBLG by adding bifunctional catalyst, 2-hydroxypyridine, in order to minimize chain scission of PBLG backbone. In this study, we conducted the aminolysis reaction at 26 °C for 24 h with 5 molar amount of 2-hydroxypyridine after preliminary experiment. Number averaged molecular weight ($M_n$) and its distribution of the starting C12–PBLG–C12 was $M_n=$ 11,800 by $^1$H NMR and $M_w/M_n=1.47$ by SEC, respectively. After the aminolysis reaction and dialysis process, we could obtain side-chain-exchanged C12–PHEG–C12 in which more than 99.2 mol% benzyl groups were exchanged by 2-hydroxyethyl groups, which was confirmed by $^1$H NMR peak area of phenyl group. $^1$H NMR and SEC measurements indicated that $M_n=9500$ and $M_w/M_n=1.71$ for C12–PHEG–C12. Degree of polymerization (DP) of PHEG was 53, and this value was identical with that for PBLG in the starting C12–PBLG–C12. Therefore, aminolysis reaction under the above condition was successful without main-chain cleavage.

### 3.2. Helix-coil transition of PHEG

CD measurements for C12–PHEG–C12 solution dissolved in water/EG mixed solvent were performed with varying EG weight fraction in the solvent ($W_{EG}$). When $W_{EG}=0$, i.e. in pure water, CD spectrum revealed that PHEG is in random-coil state as shown in Fig. 2 (-●-). With the increase of $W_{EG}$, two minima in mean residual ellipticity ([$\Theta$]) at wavelength $\lambda=208$ and 222 nm were recognized, and their absolute values were increased with $W_{EG}$. Helix content $f^H$ of PHEG was evaluated from [$\Theta$] value at $\lambda=222$ nm, $[\Theta]_{222}$ (deg cm$^2$ decimole$^{-1}$), as follows [43].

$$f^H = \frac{[\Theta]_{222}}{-40,000} \tag{7}$$

In Fig. 3, obtained $f^H$ are plotted against $W_{EG}$ by using symbol ●. The helix content was less than 10% when $W_{EG}<0.3$, and gradually increased with $W_{EG}$. Even at $W_{EG}=1.0$, $f^H$ value remained less than 0.8.

### 3.3. Association behavior in water/EG mixed solvent

Fluorescence spectra measurements of ANS-Mg, a probe molecule for fluorescence, dissolved in C12–PHEG–C12/water/EG solution with various polymer concentrations have been conducted. When polymer concentration is low, fluorescence intensity maximum is located around 500 nm. With the increase of concentration, the wavelength at the maximum shifted to the shorter wavelength and its intensity increased. These results reflect a change of surrounding circumstance around ANS: ANS molecules tend to locate in hydrophobic domain with the increase of polymer concentration. From these results, CMC of C12–PHEG–C12 can be evaluated because micellization according to association of C12 forms a hydrophobic C12 domain, in which ANS prefers to exist rather than in hydrophilic solvent. Evaluated values of CMC are plotted against $W_{EG}$ in Fig. 4. This figure shows a gradual increase in CMC with $W_{EG}$, probably

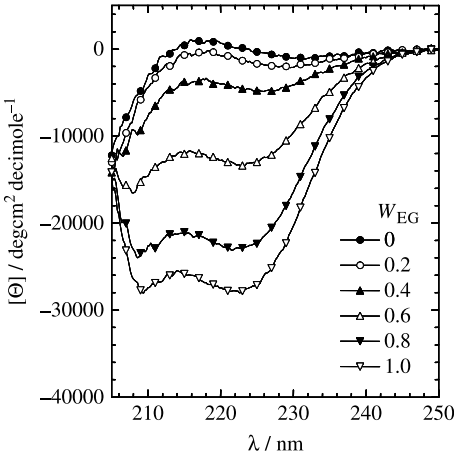


Fig. 2. CD spectra for C12–PHEG–C12/water/EG solutions with various $W_{EG}$ as indicated.

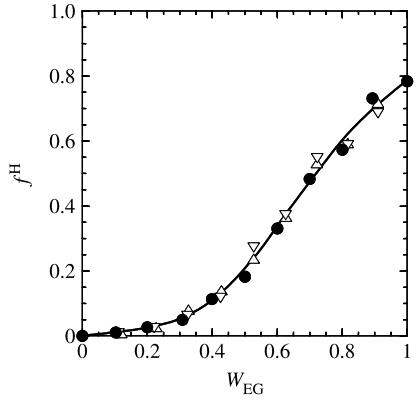


Fig. 3. Plots of $f^H$, evaluated by CD spectrum, against $W_{EG}$. (●) The sample solutions were prepared by dissolving C12–PHEG–C12 in the pre-mixed water/EG mixed solvent; (△) polymer aqueous solution was prepared at first, subsequently EG was added to make a desired $W_{EG}$ and polymer concentration; (▽) EG solution of polymer was prepared at first, then water was added into the C12–PHEG–C12/EG solution.

because association strength of C12 chain tends to be weak with increase of content of less hydrophilic EG in the solvent.

### 3.4. Light scattering

DLS measurements for C12–PHEG–C12/water/EG solutions with various $W_{EG}$ were performed. Polymer concentration for these solutions was fixed at 1.0 wt%, which is enough larger than CMC for all $W_{EG}$. As shown in typical examples in Fig. 5, obtained autocorrelation functions decay at shorter time when $W_{EG}\leq 0.5$, and for $W_{EG}\geq 0.6$ solutions, slower decay mode is dominant. These curves were analyzed by using CONTIN program, and evaluated $R_h$ distribution derived from Eq. (6), at $\theta=90°$ for various $W_{EG}$ solutions, are shown in Fig. 6. For solutions with $0\leq W_{EG}\leq 0.5$, single decay mode at $R_h\sim 7$ nm (fast mode) is observed, and with the increase of $W_{EG}$ to 0.6, the distribution profile shows drastic change and major peak locates around $R_h>100$ nm (slow mode). Similar results

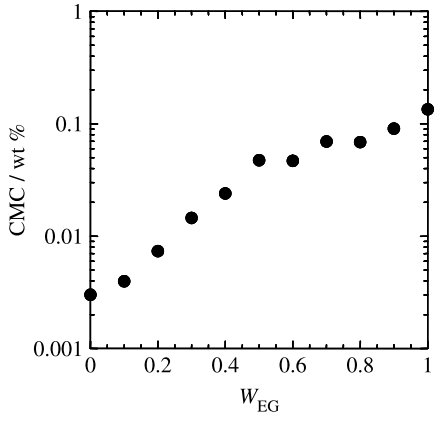


Fig. 4. Plots of critical micellar concentration (CMC) against $W_{EG}$ evaluated by fluorescence spectra.

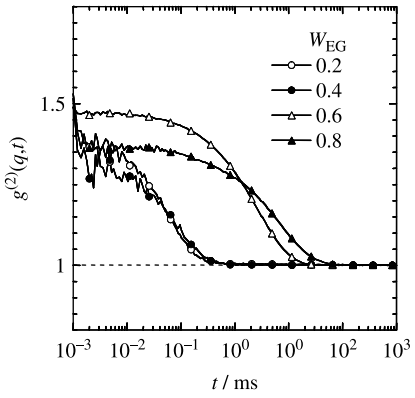


Fig. 5. Autocorrelation function of scattered light intensity $g^{(2)}(q, t)$ obtained by DLS measurements at $\theta=90°$ for C12–PHEG–C12/water/EG solutions with various $W_{EG}$ as indicated.

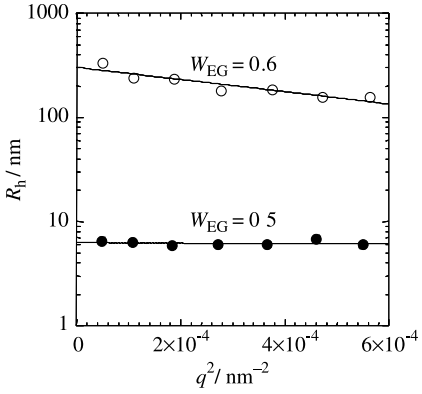


Fig. 7. Angular dependence of peak position in $R_h$ distribution curve for $W_{EG}=0.5$ (●) and 0.6 (○) solutions measured at different scattering vector $q$.

were also obtained for solutions with $0.6\leq W_{EG}\leq 0.9$. In case of pure EG solution ($W_{EG}=1.0$), scattered light intensity was too weak to evaluate $\Gamma$ distribution from autocorrelation function. As shown in Fig. 7, the fast mode shows almost identical $R_h$ for all measured scattering angles, but $R_h$ for the slow mode reveals angle dependence. Apparent hydrodynamic radius $R_{h,app}$ at finite concentration was evaluated by extrapolation to $q^2=0$, as shown by solid lines in Fig. 7, and numerical results are listed in Table 1. In Fig. 8, obtained $R_{h,app}$ for fast mode (●) and slow mode (○) are plotted against $W_{EG}$. As shown in Fig. 6, we can recognize a small slow-mode and fast-mode peak in the distribution curve for $W_{EG}=0.2$ and 0.8, respectively. However, these peaks are too weak to evaluate its position precisely, so in Fig. 8, $R_{h,app}$ values for the main peak are plotted. This plot clearly reveals that $R_{h,app}$ show gradual decrease with the increase of $W_{EG}$ when EG content is small, and drastically increase in the range of $0.5<W_{EG}<0.6$.

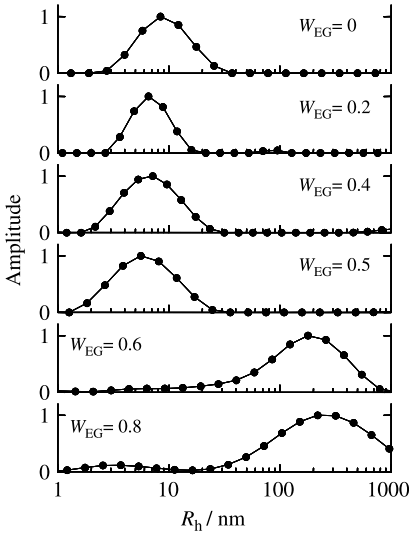


Fig. 6. Distribution of hydrodynamic radius $R_h$ evaluated by DLS measurements at $\theta=90°$ for various $W_{EG}$ solutions as indicated.

SLS measurements were also performed, and obtained Zimm-type plots are shown in Fig. 9. As shown by plots for $W_{EG}=0.2$ (●) and 0.4 (○), scattered light intensity revealed weak angular dependence when the water content is small, which means that $R_g$ of solute is small. The plot for $W_{EG}=0.5$ solution (▲) is making bended curve with larger slope in smaller angle region and almost horizontal curve in larger angle region, suggesting bimodal size distribution in solute. Increase of $W_{EG}$ to 0.6 made a sudden increase in scattered light intensity (△), indicating a formation of large associates with high molecular weight. Further increase of $W_{EG}$ induced a decrease in scattered light intensity (▽), but slope of the Zimm-type plot is larger than those for $W_{EG}\leq 0.4$. Obtained Rayleigh ratio at $\theta=45°$, $R(45°)/Kc$, are plotted against $W_{EG}$ in Fig. 10. As mentioned above, scattering light intensity drastically increased when $W_{EG}$ changed from 0.5 to 0.6, and again decreased with the further increase of $W_{EG}$. From the Zimm-type plots, $M_{w,app}$ and $R_{g,app}$ are evaluated by using Eqs. (1) and (2), and listed in Table 1. In these data analyses, slope was determined from the plot in larger angle region when $W_{EG}\leq 0.5$, and initial slope was used for solutions with $W_{EG}\geq 0.6$. It should be pointed out that the value of $R_{g,app}$ should be containing a relatively large numerical error because the slope of Zimm-type plot was close to zero. Table 1 suggests that solute

Table 1
Numerical results of light scattering measurements

| $W_{EG}$ | $R_{h,app}$/nm | $R_{g,app}$/nm | $M_{w,app}$ | $N_{app}$ |
|---|---|---|---|---|
| 0.0 | 8.7 | 18 | 138,000 | 8.5 |
| 0.1 | 8.7 | 20 | 121,000 | 7.4 |
| 0.2 | 7.4 | 10 | 125,000 | 7.7 |
| 0.3 | 6.9 | 14 | 119,000 | 7.3 |
| 0.4 | 6.6 | 20 | 82,000 | 5.0 |
| 0.5 | 6.3 | 10 | 68,000 | 4.2 |
| 0.6 | 304 | 116 | 2,900,000 | 179 |
| 0.7 | 236 | 154 | 1,130,000 | 69.6 |
| 0.8 | 456 | 233 | 311,000 | 19.1 |
| 0.9 | 351 | 165 | 86,000 | 5.3 |
| 1.0 | – | 145 | 13,000 | 0.8 |

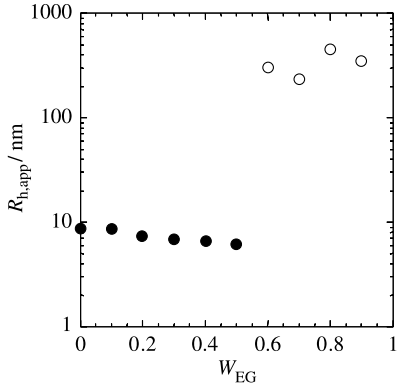


Fig. 8. Plots of $R_{h,app}$ for C12–PHEG–C12/water/EG solutions against $W_{EG}$.

particle exists in $W_{EG} \leq 0.5$ solutions have radius of ~10 nm, and $M_{w,app}$ is about 4–8 times larger than $M_w = M_n \times (M_w/M_n)$ for C12–PHEG–C12. These results indicate that C12–PHEG–C12 forms associated micelle with its association number ($N_{app}$) to be 4–8, and $N_{app}$ gradually decreases with the increase of $W_{EG}$.

## 4. Discussion

### 4.1. Structure of the associates

SLS results for C12–PHEG–C12/water solution ($W_{EG} = 0$) indicated association number of the micelle in aqueous solution is ca. 8.5. For spherical micelles in aqueous solution of HEUR with terminal dodecyl groups, number of end group in one hydrophobic domain was estimated from fluorescence measurement as 15–30 [11]. In Ref. [51], association behavior of poly(ethylene glycol) monododecyl ether (C12E25) in aqueous solution has been investigated by light scattering, and apparent association number of micelle was evaluated to be about 26. These values show good consistency with our present results, i.e. the micellar core contains $2N_{app} \approx 17$ dodecyl chains.

From $N_{app}$ and density ($\rho$) of *n*-alkyl chain, we can evaluate radius of C12-segregated core ($r_{core}$), with

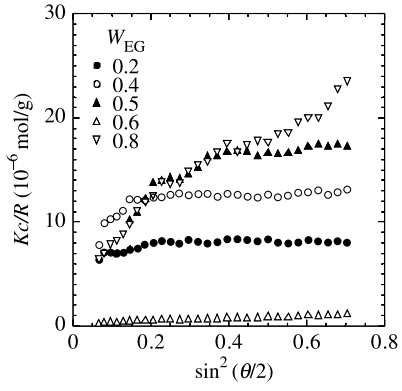


Fig. 9. Zimm-type plots of angular dependence of inverse of scattered light intensity, $Kc/R(\theta)$ vs. $\sin^2(\theta/2)$ for various $W_{EG}$ solutions as indicated.

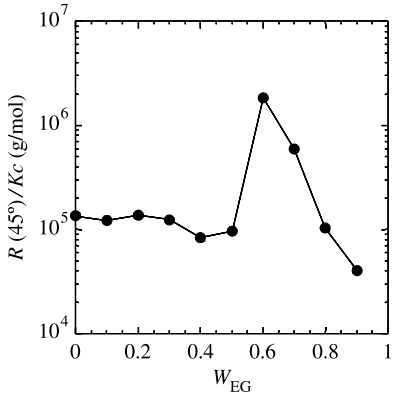


Fig. 10. $W_{EG}$ dependence of scattered light intensity at $\theta = 45°$, $R(45°)/Kc$.

assuming that the core is spherical shape and strongly rejects solvent, by using the following equation.

$$r_{core} = \left( \frac{3N_{app}M_{alkyl}}{2N_A \pi \rho} \right)^{1/3} \quad (8)$$

For $0 < W_{EG} < 0.5$ solutions, $r_{core}$ can be calculated as 0.9–1.1 nm by using parameters such as $\rho = 0.75$ (g/cm$^3$) and $M_{alkyl} = 155$ (for $-C_{11}H_{23}$ group). Mean-squared radius of gyration $\langle s^2 \rangle^{1/2}$ of PHEG homopolymer is reported to be expressed by $(6\langle s^2 \rangle)^{1/2} = \langle r^2 \rangle^{1/2} = (6.6nl^2)^{1/2}$, therefore, for PHEG with DP = 53, $\langle s^2 \rangle^{1/2}$ is calculated to be 1.9 nm. Experimental $R_{h,app}$ from DLS measurement (6.3–8.7 nm) is larger than this value, but more close to 4.7–4.9 nm calculated by simple summation such as $r_{core} + 2\langle s^2 \rangle^{1/2}$ expected for core-corona type spherical micelles as schematically represented in Fig. 11(a). As pointed out by theoretical considerations for micellar size [13,53], corona chain is probably extending along radial direction because of

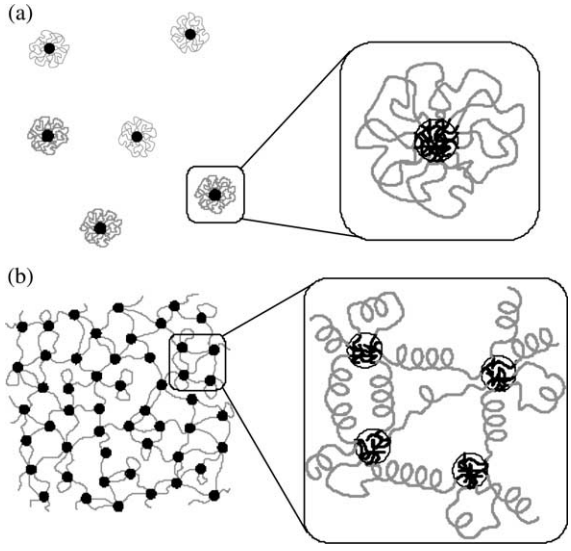


Fig. 11. Schematic representation of structure of associates. Black and dark lines represent C12 and PHEG chains, respectively. (a) Isolated flower-like micelles when $W_{EG} \leq 0.5$. (b) Large associate consisting of multiple C12 cores connected by PHEG chains with partially α-helical structure.

segmental interaction at inner region of micelle as like the case for star-like polymers. This change of chain dimension of PHEG in loop conformation will make the micellar size larger than those calculated above. Therefore, C12–PHEG–C12 is believed to be forming flower-like micelles with core-corona structure when $W_{EG} \leq 0.5$ as depicted in Fig. 11(a).

As shown in Fig. 8, $R_{h,app}$ revealed gradual decrease with the decrease in $W_{EG}$ until $W_{EG}=0.5$. One possible reason for the decrease in size is decrease in $N_{app}$, i.e. decrease of association strength of C12 with the increase of $W_{EG}$ because EG is more hydrophobic than water. Similar trend in $N_{app}$ was also reported for one-end hydrophobically modified poly(ethylene oxide) (PEO) in water/EG mixed solvent [54]. Another possible explanation is decrease in size of PHEG corona with the increase of $W_{EG}$ and its helix content $f^H$. As pointed out by Ohta et al. [47], PHEG in aqueous solution exhibited broad minimum in $\langle s^2\rangle^{1/2}$ vs. $f^H$ curve because of very low cooperativity in helix-coil transition. By using Teramoto et al.'s approximate expression for physical quantities of polypeptides [55], which was derived from Nagai's theory [56] for helix-coil transition, we can evaluate a relationship between $\langle s^2\rangle^{1/2}$ and $f^H$. In Fig. 12, result of $(\langle s^2\rangle/\langle s^2\rangle_0)^{1/2}$ against $f^H$ for PHEG with DP=53, calculated from Eqs. (23) and (24) in Ref. [55], is indicated by solid line, where $\langle s^2\rangle_0$ is equal to $\langle s^2\rangle$ at $f^H=0$. In these calculations, numerical parameters are referred from those reported by Ohta et al. [47], i.e. cooperative parameter $\sigma=0.004$, effective bond length for random coil portion $a_0=1.47$ nm, and pitch per monomeric residue in helical portion $a_1=0.197$ nm. In Fig. 12, experimental results for $R_{h,app}$ are also plotted against $f^H$. Comparison of these figures indicate that $R_{h,app}$ as well as theoretical $\langle s^2\rangle^{1/2}$ of corona chains show similar gradual decrease with the increase of $f^H$. Therefore, decrease of size of PHEG as well as $N_{app}$ are possibly contributing to the decrease of $R_{h,app}$ with the increase of $W_{EG}$.

In solutions with $W_{EG} \geq 0.6$, $R_{g,app}$ and $R_{h,app}$ are evaluated as larger than 100 nm for the slow mode, but

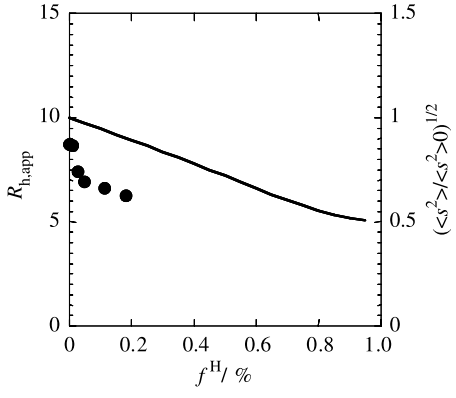


Fig. 12. Comparison of relationship of experimentally evaluated $R_{h,app}$ (●, left axis) and calculated $(\langle s^2\rangle/\langle s^2\rangle_0)^{1/2}$ for PHEG (solid line, right axis) according to Teramoto et al.'s expression [54]: DP=53, $\sigma=0.004$, $b_0=1.47$ nm, and $b_1=0.197$ nm.

$N_{app}$ decreases sharply with the increase of $W_{EG}$. It is difficult to suppose any reasonable structures of associate with small $N_{app}$ and large $R_{g,app}$ observed in large $W_{EG}$ region. So, it should be plausible that freely-dissolved C12–PHEG–C12 chains, i.e. unimer, are coexisting with large aggregate having several hundred nanometer in size. Sharp decrease of $M_{w,app}$ with maintaining large $R_{g,app}$ value may indicate that concentration of the large aggregate are decreasing with the increase of $W_{EG}$, i.e. many C12–PHEG–C12 are existing as unimer when $W_{EG}$ is large. This consideration is consistent with the decrease in $N_{app}$ with increase of $W_{EG}$ in $W_{EG}<0.5$ region, suggesting the decrease of segregation power of C12 [54]. In DLS measurement, decay of autocorrelation function by unimer is hard to be detected because of its small size.

Simple core-corona type micelle as depicted in Fig. 11(a) cannot be applicable for these large aggregates, and a network structure containing multiple C12 segregated cores connected by bridging PHEG chains as shown in Fig. 11(b) should be plausible. The sudden structure change from the isolated flower-like micelle to the large aggregate with multiple core occurred at $0.5<W_{EG}<0.6$, and in this $W_{EG}$ range, $f^H$ increased from 0.2 to 0.35. This increase in helix content of PHEG chain should be an important driving force for the structure change of associate. Larger helix content makes PHEG chain in rod-like conformation, as a result, loop conformation in which both-end C12 chains are included in the same C12 core tend to be excluded, and bridge conformation which connects different C12 cores is easily occurred. Therefore, inside of the large aggregate is expected to be a network structure, which containing multiple C12 cores connected by bridging PHEG chains with rod-like conformation. This microgel-like structure for the associate is also supported by $R_{g,app}/R_{h,app}$ value, which is usually used as a dimensionless parameter to elucidate particle structure [57,58]. Observed $R_{g,app}/R_{h,app}$ ranges 0.38–0.65, and these small values are also reported in PVA microgels with large molecular weight prepared by emulsion polymerization [57].

In order to confirm the effect of the helix-coil transition on the association behavior, both-ends hydrophobically-modified water-soluble polymer without any conformational transition is considered as a suitable control sample. Here, we comment on recent Dai et al.'s study on aggregation behavior of HEUR in water/EG mixed solvent [59]. In Ref. [59], both-ends-capped PEO ($M_n$ is 50,000) with $C_{16}H_{33}$ alkyl chains are used as HEUR, and the conformation of PEO is random coil even after the addition of EG. From light scattering and rheological measurements, they concluded that structure of HEUR associate is flower-like when EG content is low, and changes to star-like micelle with the increase of EG content, and further addition of EG induces several micelles to aggregate [59]. Although their result show some similarities with our present one, a remarkable difference between HEUR and C12–PHEG–C12 systems is that the solubility of PEO in EG is poorer than that of PHEG

(HEUR is insoluble when $W_{EG} > 0.8$, while PHEG is easily dissolved in pure EG). For HEUR, this lowering of PEO solubility is considered as the reason for the further aggregation of the micelle. Moreover, the increase of $R_h$ for HEUR aggregates with $W_{EG}$ is very gradual (from ~50 to ~120 nm when $W_{EG}$ increased from 0.3 to 0.7), while that for C12–PHEG–C12 aggregates show the sudden increase at $0.5 < W_{EG} < 0.6$. Therefore, the association mechanism proposed for HEUR cannot be applied for the increase in $R_{h,app}$ shown in Fig. 8.

In Fig. 13, distribution functions of length of helical sections, $L(n_1)$, each of which consists of $n_1$ monomeric residues, are indicated, which were calculated in accordance with Teramoto et al.'s approximate expression (Eq. (16) in Ref. [55]) with using the numerical parameters as indicated above. This figure reveals that the length of helix sequence in larger $n_1$ region increases with the increase of $f^H$, suggesting that PHEG are changing to a semi-flexible chain as pointed out above. However, because of the low cooperativity in helix-coil transition of PHEG, completely rod-like structure in which $n_1$ is close to degree of polymerization (about 50) is not obvious even when $f^H = 0.7$. We cannot recognize any significant change in the distribution curve at $f^H = 0.2$ (- - - -) and 0.35 (– – –), in between the structure of associate of C12–PHEG–C12 changed drastically. From these results, it is difficult to discuss quantitative relationship between the degree of rigidity of PHEG chain and the structure change of associate. These calculations suggest that the PHEG rigidity is influenced by not only $f^H$ but also the degree of polymerization, i.e. at the same $f^H$ value, PHEG chain is more flexible when its molecular weight becomes larger. Further experiments for C12–PHEG–C12 with various molecular weights are in progress.

### 4.2. Sample preparation dependency

In order to investigate stability of associated micelles, CD measurements were performed for sample solutions prepared by different preparation methods as follows. (1) C12–PHEG–C12 was first dissolved in pure water, and EG was added to the aqueous solution to make solutions with desired $W_{EG}$ and polymer concentration. (2) Solvent was added to polymer in reverse order, i.e. water was added to C12–PHEG–C12/EG solution prepared in advance. For solutions prepared by the methods (1) and (2), $f^H$ was elucidated by CD measurements and plotted against $W_{EG}$ in Fig. 3 (△ and ▽ for method (1) and (2), respectively). Comparison of these data with those for solutions prepared by dissolving polymer in pre-mixed water/EG solvent (● in Fig. 3) suggests that the helix content in PHEG is not influenced by solution preparation method.

Similar sample–preparation–method dependency on light scattering results was also examined. At first, DLS measurement was performed for 1 wt% polymer solution prepared from mixed solvent with $W_{EG} = 0.4$. To this solution, EG was added so as to make $W_{EG} = 0.5$ solution with lower polymer concentration, and DLS measurements was conducted after 2 days. Further addition of EG was made to obtain $W_{EG} = 0.6$ solution. $R_h$ distribution profiles for solutions prepared by this method are shown in Fig. 14(a). On the other hand, solutions with various $W_{EG}$ prepared by adding water to 1 wt% solution with $W_{EG} = 0.6$ was measured, and results are shown in Fig. 14(b). Comparison of Fig. 14(a) with Fig. 6 indicates that structure change of micelles by the addition of EG gave similar results to the solutions prepared by dissolving polymer directly in pre-mixed solvent. However, the large aggregates formed in $W_{EG} = 0.6$ solution were still observed even in $W_{EG} = 0.4$ solution prepared by the addition of water (Fig. 14(b)). From these results, we can point out that the large aggregates with bridge conformation is easily formed from the isolated flower-like micelles by the increase of

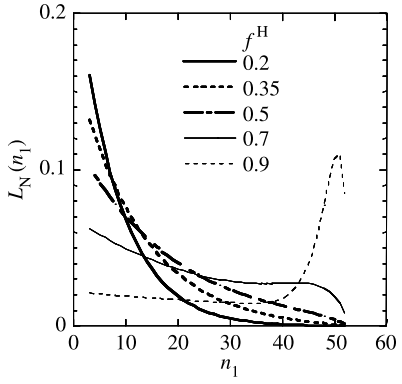


Fig. 13. Effect of helix content $f^H$ on helix sequence length distribution $L(n_1)$ for PHEG: DP = 53 and $\sigma = 0.004$.

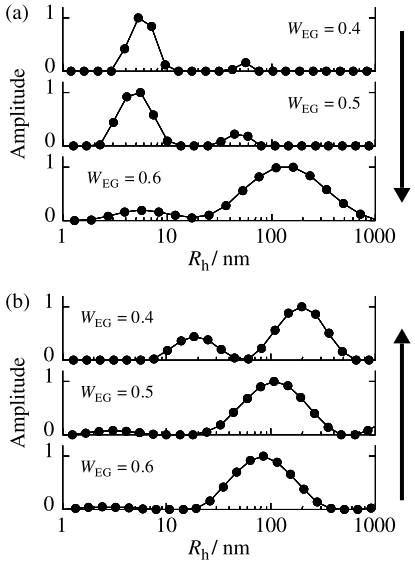


Fig. 14. Distribution of $R_h$ derived by DLS measurements. (a) Solutions of $W_{EG} = 0.5$ and 0.6 are prepared by adding EG into $W_{EG} = 0.4$ solution. (b) Water was added to $W_{EG} = 0.6$ solution to make $W_{EG} = 0.5$ and 0.4 solutions.

helix content, however, the large aggregates tend to maintain its network structure even after $f^H$ for PHEG is decreased. These dependencies on structure of associates by sample preparation process suggest a possibility to control mechanical properties of physically cross-linked gel samples of more concentrated solution. Sol–gel transition and viscoelastic measurement of moderately concentrated C12–PHEG–C12/water/EG solutions are in progress, and will be reported in future work.

## 5. Conclusions

Association behavior and its structure for C12–PHEG–C12, both-ends hydrophobically modified water-soluble polypeptide, in water/EG mixed solvent have been investigated. The middle PHEG chain is random coil state in aqueous solution, and helix content of PHEG increased with the increase of $W_{EG}$. Fluorescence measurements for dilute C12–PHEG–C12/water/EG solutions indicate formation of hydrophobic domains with the increase of polymer concentration, suggesting segregation of C12 chains in mixed solvent. Static and dynamic light scattering measurements for 1 wt% polymer concentration solutions are conducted at various $W_{EG}$. When $W_{EG}$ is less than 0.5, evaluated $R_{h,app}$ values are 6–9 nm and $N_{app}$ are 4–8, and these values are reasonable when spherical core-corona type flower-like micelle with random-coil PHEG in loop conformation is assumed. Increase of $W_{EG}$ from 0.5 to 0.6 induced drastic increase of association number and size of associate, suggesting that large aggregates in which many C12 segregated cores are connected by PHEG in bridge conformation are formed. This structure change of associate is considered to be driven by the increase of $f^H$ of PHEG chain from 0.2 to 0.35 with the increase of $W_{EG}$, which should enhance possibility to form bridge conformation by the increase of rod-like-sequence fraction. However, theoretical calculations of distribution function of length of helix section based on helix-coil transition theory [56] does not show any significant change between the distribution curves for $f^H = 0.2$ and 0.35. Solution preparation method, i.e. the order of addition of solvent, was found to influence structure of associate, especially when water was added to the solution containing larger aggregates. These differences in solution preparation process gave negligible effect on helix content of PHEG.

## Acknowledgements

We would like to acknowledge the financial support by Grant-in-Aid for Scientific Research from the Japan Society for the Promotion of Science (No. 15550105).

## References

[1] Krause S. J Phys Chem 1964;68:1948–55.
[2] Kotaka T, Tanaka T, Hattori M, Inagaki H. Macromolecules 1978;11:138–45.
[3] Balsara NP, Tirrell M, Lodge TP. Macromolecules 1991;24:1975–86.
[4] Mortensen K, Brown W, Jørgensen E. Macromolecules 1994;27:5654–66.
[5] Quintana JR, Jáñez MD, Hernáez E, Inchausti I, Katime I. J Phys Chem B 2000;104:1439–46.
[6] Zhou Z, Chu B. Macromolecules 1994;27:2025–33.
[7] Yang Y-W, Yang Z, Zhou Z-K, Attwood D, Booth C. Macromolecules 1996;29:670–80.
[8] Zhou Z, Yang Y-W, Booth C, Chu B. Macromolecules 1996;29:8357–61.
[9] Liu T, Zhou Z, Wu C, Chu B, Schneider DK, Nace VM. J Phys Chem B 1997;101:8808–15.
[10] Chassenieux C, Nicolai T, Durand D. Macromolecules 1997;30:4952–8.
[11] Alami E, Almgren M, Brown W, François J. Macromolecules 1996;29:2229–43.
[12] Elliott PT, Xing L, Wetzel WH, Glass JE. Macromolecules 2003;36:8449–60.
[13] Meng X-X, Russel WB. Macromolecules 2005;38:593–600.
[14] Yao J, Ravi P, Tam KC, Gan LH. Polymer 2004;45:2781–91.
[15] Tanaka F, Koga T. Comput Theor Polym Sci 2000;10:259–67.
[16] Monzen M, Kawakatsu T, Doi M, Hasegawa R. Comput Theor Polym Sci 2000;10:275–80.
[17] Kim SH, Jo WH. Macromolecules 2001;34:7210–8.
[18] Inomata K, Nakanishi D, Banno A, Nakanishi E, Abe Y, Kurihara R, et al. Polymer 2003;44:5303–10.
[19] Watanabe H, Kuwahara S, Kotaka T. J Rheol 1984;28(4):393–409.
[20] Sato T, Watanabe H, Osaki K. Macromolecules 1996;29(19):6231–9.
[21] Watanabe H, Sato T, Osaki K, Yao ML, Yamagishi A. Macromolecules 1997;30(19):5877–92.
[22] Watanabe H, Sato T, Osaki K. Macromolecules 2000;33(7):2545–50.
[23] Sato T, Watanabe H, Osaki K. Macromolecules 2000;33(5):1686–91.
[24] Raspaud E, Lairez D, Adam M, Carton JP. Macromolecules 1994;27(11):2956–64.
[25] Raspaud E, Lairez D, Adam M, Carton JP. Macromolecules 1996;29(4):1269–77.
[26] Lairez D, Adam M, Carton JP, Raspaud E. Macromolecules 1997;30(22):6798–809.
[27] Vega DA, Sebastian JM, Richard YL, Register A. J Polym Sci, Part B: Polym Phys 2001;39:2183–97.
[28] Dürrschmidt T, Hoffmann H. Colloid Polym Sci 2001;279:1005–12.
[29] Drzal PL, Shull KR. Macromolecules 2003;36:2000–8.
[30] Annable T, Buscall R, Ettelaie R, Whittlestone D. J Rheol 1993;37:695–726.
[31] Annable T, Buscall R, Ettelaie R. Colloids Surf 1996;112:97–116.
[32] Tam KC, Jenkins RD, Winnik MA, Bassett DR. Macromolecules 1998;31(13):4149–59.
[33] Pham QT, Russel WB, Thibeault JC, Lau W. Macromolecules 1999;32(9):2996–3005.
[34] Pham QT, Russel WB, Thibeault JC, Lau W. Macromolecules 1999;32(15):5139–46.
[35] Ng WK, Tam KC, Jenkins RD. J Rheol 2000;44(1):137–47.
[36] Tanaka F, Edwards SF. J Non-Newtonian Fluid Mech 1992;43:247–71.
[37] Tanaka F, Edwards SF. J Non-Newtonian Fluid Mech 1992;43:273–88.
[38] Tanaka F, Edwards SF. J Non-Newtonian Fluid Mech 1992;43:289–309.
[39] Tanaka F, Edwards SF. Macromolecules 1992;25(5):1516–23.
[40] Tanaka F. Polym J 2002;34(7):479–509.
[41] Nguyen-Misra M, Mattice WL. Macromolecules 1995;28:1444–57.

[42] Khalatur PG, Khokhlov AR, Kovalenko JN, Mologin DA. J Chem Phys 1999;110:6039–49.
[43] Inomata K, Itoh M, Nakanishi E. Polym J 2005;37:404–12.
[44] Lotan N, Yaron A, Berger A. Biopolymers 1966;4:365–8.
[45] Adler AJ, Hoving R, Potter J, Wells M, Fasman GD. J Am Chem Soc 1968;90:4736–8.
[46] Miyake M, Akita S, Teramoto A, Norisuye T, Fujita H. Biopolymers 1974;13:1173–86.
[47] Ohta T, Norisuye T, Teramoto A, Fujita H. Polym J 1976;8:281–7.
[48] De Marre A, Soyez H, Schacht E, Pytela J. Polymer 1994;35:2443–6.
[49] Sugimoto H, Nakanishi E, Hanai T, Yasumura T, Inomata K. Polym Int 2004;53:972–83.
[50] Itakura M, Inomata K, Nose T. Polymer 2001;42:9261–8.
[51] Yamazaki R, Inomata K, Nose T. Polymer 2002;43:3647–52.
[52] Tsierkezos NG, Molinou IE. J Chem Eng Data 1998;43:989–93.
[53] Hamley IW. The physics of block copolymers. New York: Oxford University Press; 1998 [chapter 3].
[54] Nagarajan R, Wang CC. Langmuir 2000;16:5242–51.
[55] Teramoto A, Norisuye T, Fujita H. Polym J 1970;1:55–63.
[56] Nagai K. J Chem Phys 1961;34:887–904.
[57] Burchard W. Adv Polym Sci 1983;48:1–124.
[58] Burchard W. Makromol Chem Macromol Symp 1988;18:1–35.
[59] Dai S, Sio ST, Tam KC, Jenkins RD. Macromolecules 2003;36:6260–6.